

# Dynamic trafficking patterns of IL-17-producing $\gamma\delta$ T cells are linked to the recurrence of skin inflammation in psoriasis-like dermatitis



Na Liu,<sup>a,b,c,1</sup> Hui Qin,<sup>a,b,1</sup> Yihua Cai,<sup>b,1</sup> Xia Li,<sup>a</sup> Lanqi Wang,<sup>a</sup> Qiannan Xu,<sup>a</sup> Feng Xue,<sup>a</sup> Lihong Chen,<sup>a</sup> Chuanlin Ding,<sup>b</sup> Xiaoling Hu,<sup>b</sup> David Tieri,<sup>d</sup> Eric C. Rouchka,<sup>d</sup> Jun Yan,<sup>b,\*</sup> and Jie Zheng<sup>a\*</sup>

<sup>a</sup>Department of Dermatology, Ruijin Hospital, School of Medicine, Shanghai Jiaotong University, Shanghai 200025, PR China

<sup>b</sup>Division of Immunotherapy, Department of Surgery, Immuno-Oncology Program, James Graham Brown Cancer Center, University of Louisville, Louisville, KY 40202, USA

<sup>c</sup>Department of Dermatology, Shanghai Skin Disease Hospital, School of Medicine, Tongji University, Shanghai 200443, PR China

<sup>d</sup>Department of Biochemistry and Molecular Genetics, University of Louisville, Louisville, KY 40202, USA

## Summary

**Background** Psoriasis recurrence is a clinically challenging issue. However, the underlying mechanisms haven't been fully understood.

**Methods** RNAseq analysis from affected skin of psoriatic patients treated with topical glucocorticoid (GC) with different outcomes was performed. In addition, imiquimod (IMQ)-induced mouse psoriasis-like model was used to mimic GC treatment in human psoriasis patients. Skin tissues and draining and distant lymph nodes (LNs) were harvested for flow cytometry and histology analyses.

**Findings** RNAseq analysis revealed that chemokine and chemokine receptor gene expression was decreased in post-treated skin compared to pre-treated samples but was subsequently increased in the recurred skin. In IMQ-induced mouse psoriasis-like model, we found that  $\gamma\delta$ T17 cells were decreased in the skin upon topical GC treatment but surprisingly increased in the draining and distant LNs. This redistribution pattern lasted even two weeks post GC withdrawal. Upon IMQ re-challenge on the same site, mice previously treated with GC developed more severe skin inflammation. There were  $\gamma\delta$ T17 cells migrated from LNs to the skin. This dynamic trafficking was dependent on CCR6 as this phenomenon was completely abrogated in CCR6-deficient mice. In addition, inhibition of lymphocyte egress prevented this heightened skin inflammation induced by IMQ rechallenge.

**Interpretation** Redistribution of pathogenic  $\gamma\delta$ T17 cells may be vital to prevent disease recurrence and this model of psoriasis-like dermatitis.

**Funding** This work was supported by National Natural Science Foundation of China 81830095/H1103, 81761128008/H10 (J.Z.) and the NIH R01AI128818 and the National Psoriasis Foundation (J.Y.).

**Copyright** © 2022 The Author(s). Published by Elsevier B.V. This is an open access article under the CC BY-NC-ND license (<http://creativecommons.org/licenses/by-nc-nd/4.0/>)

**Keywords:** Psoriasis;  $\gamma\delta$  T cells; Migration; IL-17; Skin inflammation; CCR6

## Introduction

Psoriasis is an autoimmune chronic inflammatory skin disease affecting approximately 2% of population worldwide.<sup>1</sup> The common challenge for psoriasis treatment including conventional topical glucocorticoid (GC)

treatment and many newly approved biologics is eventually disease recurrence in weeks or months interval after drug withdrawal.<sup>2–5</sup> Intriguingly, when disease recurs, the appearance of new lesions is often in the place of previous ones, suggesting immune memory involvement.<sup>6</sup> It was thought that psoriasis-specific Th17/Tc17 cells and tissue resident memory T cells (T<sub>RM</sub>) play critical roles in this process.<sup>7–10</sup> In addition to adaptive T cells, innate  $\gamma\delta$  T cells are also thought to be involved in psoriasis immunopathogenesis.<sup>11,12</sup> Previous studies have showed that dermal  $\gamma\delta$  T cells are the major

\*Corresponding authors.

E-mail addresses: [jun.yan@louisville.edu](mailto:jun.yan@louisville.edu) (J. Yan), [jie.zheng2001@126.com](mailto:jie.zheng2001@126.com) (J. Zheng).

<sup>1</sup> These authors contributed equally to this work.

eBioMedicine 2022;82:  
104136  
Published online xxx  
<https://doi.org/10.1016/j.ebiom.2022.104136>

### Research in context

#### *Evidence before this study*

Psoriasis is a skin autoinflammatory disease with no cure. One of the most challenging aspects of treating psoriasis is the tendency of psoriatic lesions to recur after treatment is discontinued. Previous studies have implicated that psoriasis specific Th17/Tc17 cells and tissue resident memory T cells ( $T_{RM}$ ) play critical roles in disease recurrence. In addition, innate  $\gamma\delta$  T cells are also thought to be involved in psoriasis pathogenesis. However, how these cells involve in disease recurrence and the underlying mechanisms remain largely unexplored.

#### *Added value of this study*

Our findings suggest that trafficking pattern changes of pathogenic  $\gamma\delta$ T17 cells play a critical role in skin inflammation recurrence in psoriasis-like dermatitis.  $\gamma\delta$ T17 cell dynamic trafficking between skin and draining and distant lymph nodes is dependent of CCR6.

#### *Implications of all the available evidence*

Our study suggests inhibition of pathogenic  $\gamma\delta$ T17 cell redistribution as an effective treatment to prevent disease recurrence in patients with psoriasis and in psoriasis-like dermatitis.

cellular source of IL-17 in the mouse skin and play a critical role in imiquimod (IMQ)-induced psoriasis-like skin inflammation and human psoriatic pathogenesis.<sup>11,13,14</sup> Interestingly, innate  $\gamma\delta$  T cells are also shown to bear “memory” phenotype.<sup>15,16</sup> Despite these studies, how these cells involve in disease recurrence and the underlying mechanism remain elusive.

A previous study using lesional skin but now normal-appearing skin upon TNF- $\alpha$  antagonist antibody (Ab) treatment has revealed that a set of inflammation-related genes remain elevated in treated lesions.<sup>17</sup> In addition, genes related to lymphatic vessels and skin structural cell types are also altered. These correlative analyses provide insights into understanding psoriasis recurrence. To further dissect the mechanism underlying disease recurrence, we recruited a cohort of psoriatic patients who received topical GC treatment. Lesional skin before GC treatment was biopsied from all patients (pre-treated). Patients who had effective treatment also had skin biopsy (post-treated). A fraction of patients had recurrence and skin biopsy was again performed (recurrent). Through unbiased RNA sequencing (RNA-Seq) analysis from these skin tissues, we found that chemokine/chemokine receptor gene expression such as CCL20 was decreased in post-treated skin compared to that in pre-treated lesional skin but subsequently increased in the recurred skin. These findings led us to hypothesize that differential trafficking patterns of

pathogenic IL-17-producing cells in psoriasis may play a critical role in disease recurrence. IMQ-induced psoriasis-like mouse model has been extensively studied and this model recapitulates some markers of human psoriasis such as skin histopathology.<sup>11,18</sup> We modified this model to help dissect potential cellular etiology underlying psoriasis recurrence. We found that innate IL-17-producing  $\gamma\delta$  T cells ( $\gamma\delta$ T17) were initially increased in dermis upon disease induction by IMQ but surprisingly migrated into draining and distant lymph nodes (LNs) after effective GC treatment.  $\gamma\delta$ T17 cells persisted for a long time and then quickly trafficked back to the inflamed skin to induce the heightened skin inflammation, mimicking human psoriasis recurrence. This process was dependent on CCR6, and inhibition of lymphocyte egress abrogated the heightened skin inflammation. Collectively, these data suggest that the trafficking pattern changes of pathogenic  $\gamma\delta$ T17 cells may hold the key in regulating disease recurrence in this model of psoriasis-like dermatitis.

## Methods

### Human subjects

Twenty-one patients (age, 27-69 years old) with psoriasis vulgaris were recruited. Peripheral blood (PB) and skin biopsies of patients were taken. Patient demographics and clinical characteristics were summarized in the Supplemental Table 1. Detailed psoriasis area and severity index (PASI) scores from each patient and information related to previous treatments in these patients were summarized in Supplemental Table 2. None of the patients had been treated with systemic drugs for at least 4 weeks and had not been treated with topical drugs other than emollients at least 2 weeks prior to the study entry. The study was approved by the Shanghai Jiaotong University Ruijin Hospital Ethics Committee (IRB#1.1/2014-10-13). All the participants gave their written informed consent.

### Patient treatment

All patients received the topical treatment of Halometasone cream (GC, Hong Kong Bright Future Pharmaceuticals) once daily for 2 weeks. Halometasone was withdrawn for 4 weeks and then assessed the severities of psoriatic lesions by PASI. One patient was excluded due to loss of follow-up. All other patients completed the schedule. PB and approximate 8 mm skin biopsy were taken at the typical lesion areas before treatment, after treatment and 4 weeks after GC withdrawal. A total of 11 patients experienced episodes of effective treatment then recurrence. Half of the biopsy tissues was used for histology and immunofluorescent staining and the other half of tissue was used for RNA extraction.

The biopsy tissues from additional three patients were used for flow cytometry analysis.

### Mice

Wildtype (WT) C57BL/6 mice (RRID:IMSR\_JAX:000664), *Tcrd*<sup>-/-</sup> (RRID:IMSR\_JAX:002120), *Ccr6*<sup>-/-</sup> (RRID:IMSR\_JAX:005793) and *Ccr2*<sup>-/-</sup> mice (RRID:IMSR\_JAX:004999) on C57BL/6 background were purchased from Jackson Laboratory and bred at the University of Louisville animal facility. All animals were housed and treated in accordance with institutional guidelines and approved by the Institutional Animal Care and Use Committee (IACUC) at the University of Louisville.

### Mouse treatments

WT, *Tcrd*<sup>-/-</sup>, *Ccr6*<sup>-/-</sup>, and *Ccr2*<sup>-/-</sup> mice between 6 and 8 weeks of age were divided into Vas control group and GC treatment group. Mice were treated daily for 5 days on each ear with 10mg of 5% imiquimod cream (3M Health Care Limited) to induce psoriasis-like inflammation. From Day 6, GC group mice were treated with 10mg Halometasone on each ear every day for 16 days along with IMQ topical treatment. Mice treated with Vaseline (Vas) were used as controls. After Halometasone or Vas treatment, all mice rested for 2 weeks. Mice were then re-challenged with IMQ for 7 days. Skin tissue, cervical LNs and inguinal LNs were harvested on Day 21, Day 35 and Day 42, respectively. For adoptive transfer experiment, cervical LNs from Vas- or GC-treated mice on day 35 were harvested and  $\gamma\delta$  T cell were isolated with TCR $\gamma\delta$  T cell isolation kit (Miltenyi, Cat # 130-092-125). Total 140,000  $\gamma\delta$  T cells were adoptively transferred into naive mouse (6-8 weeks) through retroocular vein. Recipient mice were then challenged with IMQ for 7 days. Mice were euthanized on day 8. For IMQ application on the different ear during rechallenge phase, mice were treated daily for 5 days on the left ear with 10mg of 5% imiquimod cream. From day 6, mice were treated with 10mg GC on the same site every day for 16 days along with IMQ topical treatment. Mice treated with Vas were used as controls. After GC or Vas treatment, all mice rested for 2 weeks. Mice were then re-challenged with IMQ on day 35 for 7 days on the right ear. Mice were euthanized on day 42. For FTY720 inhibitor experiments, mice received 1mg/kg FTY720 (Sigma) in normal saline by intraperitoneal (i.p) injection one day before IMQ re-challenge, dosed every day during the course of IMQ re-challenge. Ear thickness was measured everyday with digital caliper (Mitutoyo).

### A single cell suspension preparation

Human skins were incubated in dispase (BD Biosciences) for 2 h at 37°C and epidermis and dermis were separated. Human dermis and mouse ear skin tissues were

cut into small pieces and digested for 2 hours at 37°C with rotation in complete RPMI640 medium containing 1%FBS, 1 mg/mL collagenase type IA, 50  $\mu$ g/mL DNaseI and 400  $\mu$ g/mL Hyaluronidase (all from Sigma) and then filtered through 40  $\mu$ m (mouse) or 100  $\mu$ m (human) cell strainers. Human PBMCs were separated by density gradient centrifugation using Ficoll paque premium (GE healthcare), according to the manufacturer's instruction. Cervical LNs and inguinal LNs from mice were also harvested to prepare single-cell suspensions.

### Flow cytometry analysis and intracellular staining

Fluorochrome-labeled mAbs including anti-mouse CD3 (17A2, RRID: AB\_1595492),  $\gamma\delta$ TCR (GL3, RRID: AB\_1595492), V $\gamma$ 4 (UC3-10A6, RRID: AB\_10569353), V $\delta$ 4 (GL2, RRID: AB\_1877234), CD45 (30-F11, RRID: AB\_312973), CD11b (M1/70, RRID: AB\_312791), Gr-1 (RB6-8C5, RRID: AB\_313377), and IL-17A (TC11-18H10.1, RRID: AB\_2125010) and IL1R1 (DIH9, RRID: AB\_2687367) were purchased from Biolegend. Anti-human  $\gamma\delta$ TCR (REA591, Cat # 130-113-508) was purchased from Miltenyi Biotec and anti-human CD3 (UCHT1, Cat # 550795) was purchased from BD bioscience. For intracellular IL-17 staining, mouse skin cells or LN cells were treated with GolgiPlug (Biolegend) at 37°C for 4 h. Cells were first blocked with anti-CD16/32 and then stained with different cell surface Abs at 4°C for 20 min. Cells were then fixed, permeabilized and stained intracellularly at 4°C overnight for IL-17A. The relevant isotype control mAbs were also used. Samples were harvested with BD FACS Canto and analyzed with FlowJo software (TreeStar).

### RNA isolation

Skin biopsy tissues were placed in Trizol (Ambion, Foster City, CA) and stored at -80°C for further processing. In brief, tissue samples were placed in 2 ml tubes (axxygen, Corning) along with three stainless steel balls and run through tissue lyser (Jingxin, Shanghai, China) 60HZ with 60s for 3-6 times until the tissues were completely grinded. RNA was extracted using the Eastep<sup>®</sup> Super Total RNA Extraction Kit (Promega, Shanghai, China) based on manufacturer instructions.

### Real time quantitative polymerase chain reaction (qRT-PCR)

Isolated RNA was reverse transcribed into cDNA with a Reverse Transcription Kit (Takara, Shiga Japan). qRT-PCR was performed using SYBR Green Master (Roche, Basel, Switzerland) according to the manufacturer's instructions and gene-specific primers were summarized in the Supplemental Table 3. qRT-PCR was done on an Applied Biosystems 7500. We normalized gene expression amount to GAPDH (human) or  $\beta$ -MG

(mouse) housekeeping genes and represented data as fold changes by the  $\Delta\Delta Ct$  method.

### RNA-Seq

Total RNA was extracted and library was constructed and sequenced with sequencing platform BGISEQ-500 (BGI). The sample sequences were directly aligned to the *Homo sapiens* hg38 reference genome assembly using tophat2 (version 2.0.13), generating alignment files. The number of reads was between 37 to 52 million. The alignment rate ranged from 88-93% across the samples from the left read, and 76-88% for the right read, resulting in a concordant mapping rate of 72-83%. Quality control of the raw sequence data was performed using FastQC (version 0.10.1). For the first read, the interquartile range remained above 30 (99.9% base call accuracy); across the reads. Differential expression analysis was performed using the Tuxedo Suite program cuffdiff2 (version 2.2.1). A q-value cutoff  $\leq 0.05$  with  $|FC| \geq 1$  was used to determine differential expression. RNA-Seq data have been deposited into NCBI GEO with the accession number (GSE114729).

### Skin histology

Fresh human and mouse skin samples were fixed in 4% paraformaldehyde solution for 24h, dehydrated, and embedded in paraffin. Tissue sections ( $\sim 10\mu\text{m}$  in thickness) were used for various staining. For histopathology, human and mice sections were stained with hematoxylin and eosin (H&E). The ear skin from WT and *Tcrd*<sup>-/-</sup> mice was dissected and frozen in optimal cutting temperature (OCT) compound. Sections ( $10\mu\text{m}$  thick) were cut with a cryostat. The slides were stained with hematoxylin and eosin for morphology and cellular infiltration. Images were acquired at  $\times 200$  magnification using Aperio ScanScope digital scanners.

### Immunofluorescence staining

For immunofluorescence, the ear skin from WT and *Tcrd*<sup>-/-</sup> mice was dissected and frozen in optimal cutting temperature (OCT) compound. Sections ( $10\mu\text{m}$  thick) were cut with a cryostat. After fixation with cold acetone for 30 min, slides were blocked with 20% FBS in PBS for 60 min at room temperature, and then stained with anti-mouse Gr-1 (RB6-8C5, 1:100, Biolegend) in 20% FBS at 4 °C overnight. Nuclei were visualized by DAPI (1  $\mu\text{g}/\text{ml}$ , Invitrogen, USA) staining for 10 min. Images were acquired by Nikon confocal microscope system.

### Statistics

Differences between two sets of data were evaluated by 2-tailed Student's t-test. For more than two groups, we used nonparametric multiple testing methods with

human data while one-way or two-way ANOVA was used for mouse data analysis. Data represent as mean and error or mean  $\pm$  SEM as indicated.  $P \leq 0.05$  was considered statistically significant. All statistics were done using GraphPad Prism (GraphPad Software).

### Role of funders

The Funders had no roles in study design, data collection, data analyses, interpretation or writing of report.

## Results

### Skin tissues from psoriasis patients show fluctuated chemokine levels that are correlated with different disease episodes

To investigate the possible etiology underlying psoriasis recurrence, GC was topically applied on the lesional skin for 2 weeks and then withdrawn. A total 11 patients experienced episodes of effective treatment and then recurrence. Skin tissues (pre-treated, post-treated, and recurrent) from these patients were obtained and subjected to RNA-Seq analysis. Upon effective treatment with GC, many genes and pathways related to psoriasis pathogenesis including TCR pathway, keratinocyte pathway, and positive regulation of innate immune response were downregulated (Figure S1a, S1c). In contrast, when disease recurred, these genes and pathways were upregulated or enriched (Figure S1b, S1d). In addition, the mRNA expression levels of IL-17 and IL-23 were also decreased post GC treatment while upregulated after disease relapse (Figure S1e). Notably, lymphocyte chemotaxis pathway including chemokine/chemokine receptor genes was among this list (Figure 1a), including CCL20, CCL5, and CXCL10. These gene expression levels in the skin from different disease stages were also validated by qRT-PCR analysis (Figure 1b). CCL20 is a ligand for CCR6 which is expressed on all IL-17-producing T cells (T17), supporting critical roles of IL-17 played in psoriasis pathogenesis, treatment response, and disease recurrence. Since a previous study reported that proinflammatory human skin-homing V $\gamma$ 9V $\delta$ 2 T cells are associated with psoriasis treatment response,<sup>19</sup> we thus examined CD3<sup>+</sup> T cells and innate  $\gamma\delta$  T cells in the skin and peripheral blood (PB) during GC treatment. Upon effective GC treatment, skin infiltrating CD3<sup>+</sup> T cells were decreased and so were dermal  $\gamma\delta$  T cells (Figure 1c and 1e). When disease recurred, CD3<sup>+</sup> T cells as well as  $\gamma\delta$  T cells were increased in the lesional skin. In contrast,  $\gamma\delta$  T cells in the PB experienced an opposite wave as compared to skin-infiltrating  $\gamma\delta$  T cells. Circulating  $\gamma\delta$  T cells were increased upon effective GC treatment while decreased when disease recurred (Figure 1d, 1f and 1g) although total CD3<sup>+</sup> T cells in the PB did not follow this trend. This was revealed by both fold changes and absolute

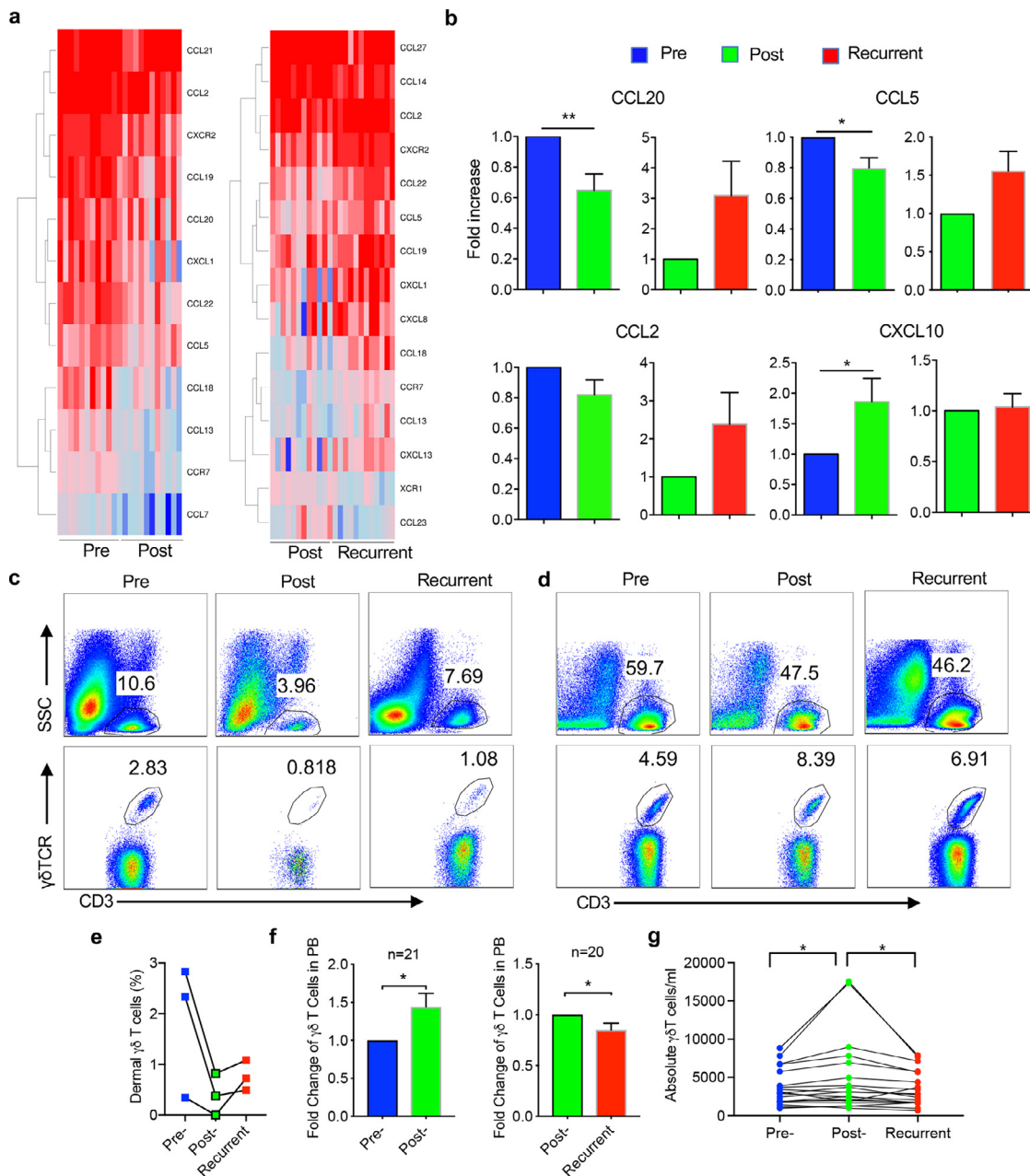


**Figure 1. Differential chemokine/chemokine receptor gene expression profiles by RNAseq analysis and  $\gamma\delta$  T cells in human psoriasis patients.** (a) Heatmaps show the differentially expressed chemokines/chemokine receptors genes in the pre- versus post-treated skins and post-treatment versus recurrent skins. (b) The mRNA expression levels of CCL20, CCL5, CCL2, and CXCL10 assessed by real-time PCR analysis in the pre-, post-, and recurrent skins ( $n=21$ ).  $*P<0.05$ ,  $**P<0.01$  (nonparametric multiple test). (c) Skin biopsies from pre-, post- and recurrent patients were stained with CD3, pan  $\gamma\delta$ TCR, and viability dye. Cells were gated on viable (upper) or CD3<sup>+</sup> cells (lower). Representative flow plots are shown. (d) PB sample obtained from the same patient in panel c was stained with CD3 and pan  $\gamma\delta$ TCR. Cells were gated on total PBMC or CD3<sup>+</sup> cells. Representative flow plots are shown. (e) Summarized percentages of dermal  $\gamma\delta$  T cells in skin tissues from three pre-, post-treatment, and recurrent psoriatic patients. (f) Fold changes of PB  $\gamma\delta$  T cells from patients before and after treatment ( $n=21$ ) and post-treatment and recurrent ( $n=20$ ) are shown.  $*P<0.05$  (paired Student's t test). (g) Absolute numbers of  $\gamma\delta$  T cells in 1ml PB from patients before and after treatment ( $n=21$ ) and post-treatment and recurrent ( $n=20$ ) are shown.  $*P<0.05$  (paired Student's t test). Data in the bar figures are represented as means $\pm$ SEM.

numbers (Figure 1f and 1g). These findings suggest that trafficking changes of T cells, particularly innate  $\gamma\delta$  T cells may be associated with disease resolution and recurrence in psoriasis.

#### IMQ-induced psoriasis-like skin inflammation is ameliorated upon GC treatment with decreased $\gamma\delta$ T17 cells in the skin but increased in the distant LNs

To delineate the mechanisms underlying psoriasis recurrence, we used a well-established IMQ-induced psoriasis-like dermatitis model to mimic human psoriasis pathogenesis and treatment schedule. To this end, IMQ was topically applied on mouse ear skin for 3 weeks. Starting at day 6, inflamed skin was treated with GC or Vas. Treatment was completed on day 21 and mice were rested for 2 weeks and then re-challenged with IMQ for 7 days (Figure 2a). On day 21, mice treated with GC had significantly decreased ear thickness compared to Vas control (Figure 2b left), mimicking effective GC treatment in human psoriasis patients. Consistent with previous reports,<sup>11,14</sup> ear thickness was significantly lower in TCR  $\delta$ -deficient (*Tcrd*<sup>-/-</sup>) mice (Figure 2b right), suggesting critical role of  $\gamma\delta$  T cells in this model system. This was also confirmed by skin histology analysis (Figure 2c). We then extensively phenotyped T cells in the skin and draining and distant LNs from these mice by flow cytometry. The gating strategy for the skin tissues (Figure S2a) and LNs (Figure S2b) is shown in Figure S2. GC treatment drastically reduced CD3<sup>+</sup> T cells in the skin (Figure S3a), similar to psoriatic patients. Dermal  $\gamma\delta$  T cells, particularly V $\gamma$ 4V $\delta$ 4 T cells were significantly decreased in GC treated mice (Figure S3a). Immunofluorescence staining and flow analysis revealed that inflammatory neutrophil infiltration was also diminished in GC-treated skin (Figure 2d). However, no difference was observed in *Tcrd*<sup>-/-</sup> mice. Since  $\gamma\delta$  T cells are the major cellular source of IL-17 in mice,<sup>11</sup> we thoroughly examined  $\gamma\delta$ T17 cells in the skin and skin draining cervical LNs and distant inguinal LNs. Consistent with disease progression, GC-treated mice had drastically decreased IL-17 production from CD3<sup>+</sup> T cells,  $\gamma\delta$  T cells, V $\gamma$ 4 T cells, and V $\gamma$ 4V $\delta$ 4 T cells in the skin even without re-stimulation *ex vivo* (Figure 2e). This was not only by percentage but also by absolute number (Figure 2e). In the skin draining cervical LNs, we noticed that although  $\gamma\delta$  T cell percentage was decreased in GC-treated mice, V $\gamma$ 4 T cells were higher in these mice (Figure S3b). Intriguingly, V $\gamma$ 4 T and V $\gamma$ 4V $\delta$ 4 T cells even produced more IL-17 than those from Vas control mice (Figure 2f). However, the absolute  $\gamma\delta$ T17 cells and V $\gamma$ 4V $\delta$ 4 T17 cells in GC-treated mice were still lower than those from Vas control mice (Figure 2f). This was even more striking in the distant inguinal LNs. Both total percentages of  $\gamma\delta$  T cells, V $\gamma$ 4 T cells, and V $\gamma$ 4V $\delta$ 4 T cells (Figure S3c) and the percent of IL-17 production from these cells were significantly

increased in GC-treated mice compared to these in Vas control mice (Figure 2g). In addition, the absolute number of IL-17-producing  $\gamma\delta$  T cells and V $\gamma$ 4 T cells was also significantly increased (Figure 2g). In contrast, CD3<sup>+</sup> $\gamma\delta$ <sup>-</sup> T cells produced minimal IL-17 and no difference was noticed in the skin draining and distant LNs although Th17 cells were lower in the skin in GC-treated mice (Figure S3d). Interestingly, IL-1R expression levels on dermal  $\gamma\delta$  T cells, V $\gamma$ 4 T cells, and V $\gamma$ 4V $\delta$ 4 T cells were significantly increased in GC-treated mice (Figure S3e). Upregulation of IL-1R is found to be associated with memory V $\gamma$ 4 T17 cells in skin inflammation.<sup>16</sup> These data suggest that decreased  $\gamma\delta$ T17 cells in the GC-treated inflamed skin may migrate into skin draining and distant LNs with memory phenotype.

#### $\gamma\delta$ T17 cells persist in the draining and distant LNs after GC treatment withdrawal

To mimic human psoriasis patient's treatment schedule, these mice were rested for 2 weeks after GC treatment. Ear thickness in Vas control mice was gradually decreased over time (Figure 3a). This was also confirmed by skin histology (Figure 3b). However, skin-infiltrating neutrophils were found surprisingly to be more in the GC-treated mice compared to Vas control mice although no difference was observed in *Tcrd*<sup>-/-</sup> mice (Figure 3c). The frequency and absolute number of total dermal  $\gamma\delta$ T17 cells and IL-17-producing V $\gamma$ 4 and V $\gamma$ 4V $\delta$ 4 T cells remained significantly lower in GC-treated mice (Figure 3d) compared to those in Vas-treated control mice. In contrast, IL-17 production from these cells in draining and distant LNs of GC-treated mice, both frequency and absolute number, was still significantly higher than those in Vas control mice (Figure 3e, f). It appears that  $\gamma\delta$ T17 cells remain accumulated in the draining and distant LNs after GC treatment withdrawal for 2 weeks.

#### Rechallenge of previously GC-treated mice on the same site drives $\gamma\delta$ T17 cell trafficking from LNs to the dermis resulting in a heightened inflammation

We next re-challenged these mice with IMQ on the same ear to mimic human psoriasis recurrence. After three days of IMQ application, the changes of ear thickness from previously GC-treated mice were significantly higher than Vas control mice (Figure 4a left). However, this phenomenon was reversed in *Tcrd*<sup>-/-</sup> mice (Figure 4a middle). Similarly, fold changes of epidermal thickness also showed significantly increase in these mice although no difference was seen in *Tcrd*<sup>-/-</sup> mice (Figure 4a right). This was also confirmed with skin histology analysis (Figure 4b). More neutrophils were accumulated in the previously GC-treated mouse skin as revealed by both immunofluorescent staining and flow cytometry (Figure 4c). This was opposite in *Tcrd*<sup>-/-</sup>

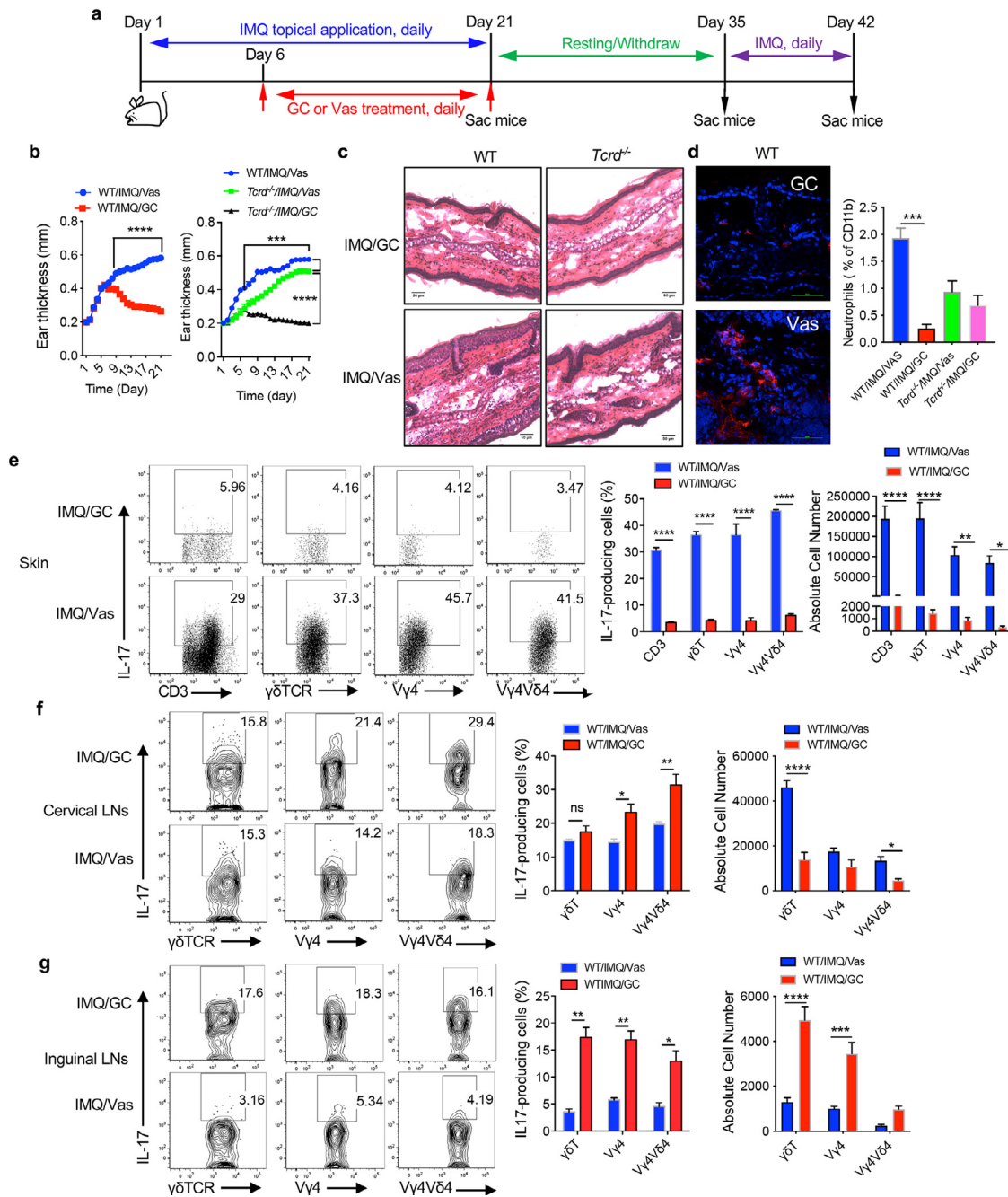


**Figure 2. GC treatment reduces skin inflammation and drives  $\gamma\delta$ T17 cells from skin to the draining and distant LNs.** (a) Schema for mouse model establishment. (b) Mouse ear thickness was measured daily from Day 1 to Day 21. (Left) Ear thickness from WT/IMQ/Vas and WT/IMQ/GC groups ( $n=24$  in each group). Data are the combination of two experiments and represent as mean and error.  $****P<0.0001$  (unpaired Student's t test). (Right) Ear thickness from WT/IMQ/Vas,  $Tcrd^{-/-}$ /IMQ/Vas, and  $Tcrd^{-/-}$ /IMQ/GC groups ( $n=5$  in each group).  $***P<0.001$  (one-way ANOVA) (c) Representative HE stained skin sections of WT and  $Tcrd^{-/-}$  mice on Day 21, scale bar= $50\ \mu\text{m}$ . (d) Representative immunofluorescence stained skin sections of WT mice treated with GC or Vas on Day 21 (Gr-1, red; DAPI, blue). Scale bar= $50\ \mu\text{m}$ . (Right) Summarized neutrophil percentages assessed by flow cytometry (WT  $n=5$ ,  $Tcrd^{-/-}$   $n=3$ ) are shown. Cells were gated on  $CD45^+CD11b^+$  cells.  $***P<0.001$  (one-way ANOVA). (e-g) IL-17 production by CD3,  $\gamma\delta$  T,  $V\gamma 4$ , and  $V\gamma 4V\delta 4$  T cells from skin (e), cervical LNs (f), and inguinal LNs (g) ( $n=5$  in each group) on day 21. Representative flow plots and absolute number are shown. Cells were gated on CD3,  $\gamma\delta$ TCR,  $V\gamma 4$ ,  $V\gamma 4V\delta 4$  T cells, respectively. Data are representative of at least two independent experiments with similar results.  $****P<0.0001$ ,  $***P<0.001$ ,  $**P<0.01$ ,  $*P<0.05$  (unpaired Student's t test). Data in the bar figures are represented as means $\pm$ SEM.

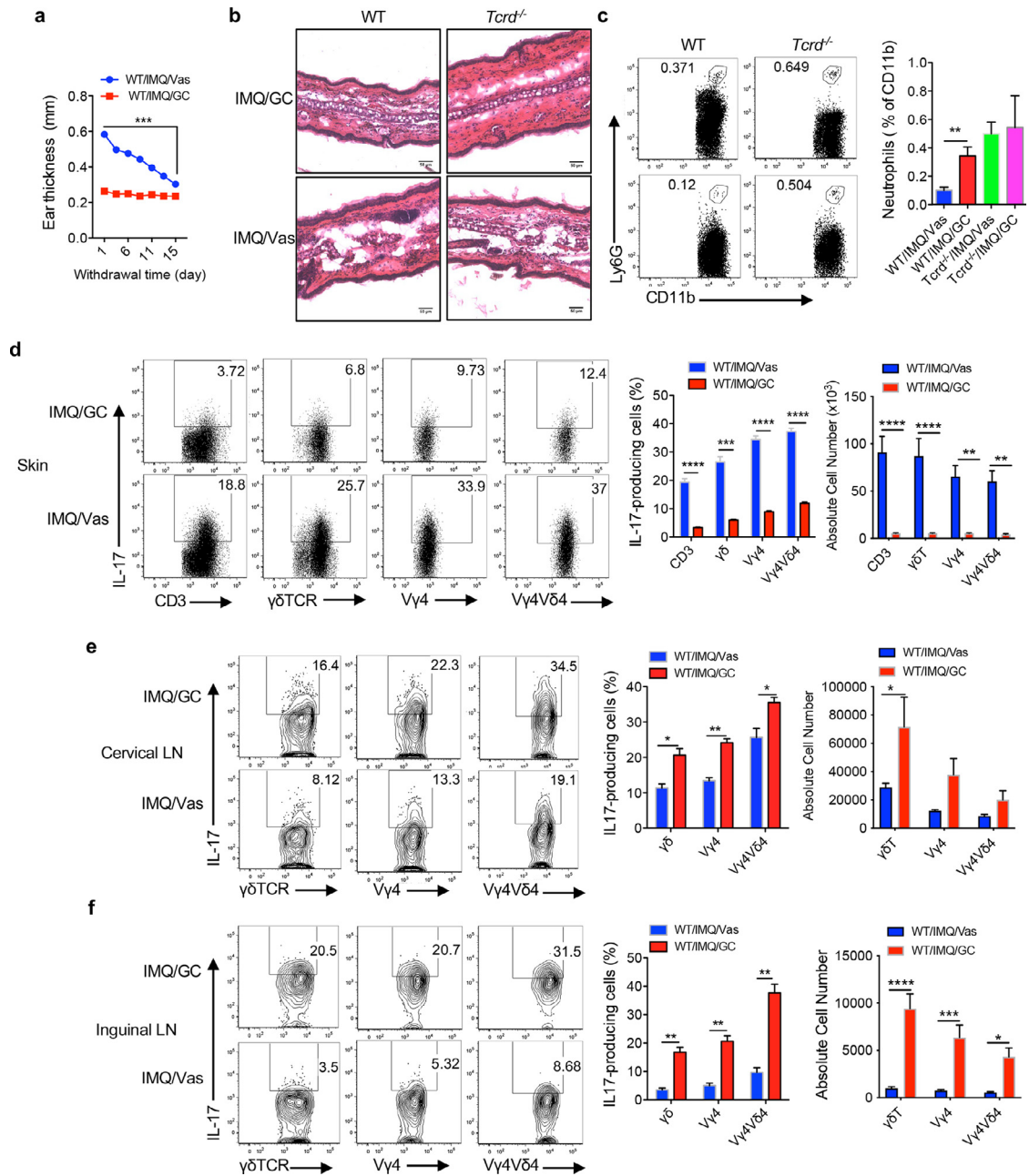


**Figure 3. GC treatment withdrawal maintains the distribution patterns of  $\gamma\delta$ T17 cells in the skin and draining and distant LNs.** (a) Ear thickness of WT mice from Day 21 to Day 35. Data are the combination of two experiments ( $n=14$ ) and represent as mean and error.  $***P<0.001$  (unpaired Student's t test). (b) Representative HE stained skin sections of WT and *Tcrd*<sup>-/-</sup> mice on Day 35, scale bar=50  $\mu$ m. (c) Neutrophil infiltration. Representative flow plots and summarized percentages are shown. Cells were gated on CD45<sup>+</sup>CD11b<sup>+</sup> cells (WT  $n=9$ , *Tcrd*<sup>-/-</sup>  $n=3$ ). Data are representative of at least two independent experiments with similar results.  $**P<0.01$  (one-way ANOVA). (d-f) IL-17 production by CD3<sup>+</sup>, dermal or LNs  $\gamma\delta$  T, V $\gamma$ 4 T, V $\gamma$ 4V $\delta$ 4 T cells from skin (d), cervical LNs (e) or inguinal LNs (f) on day 35. Flow plots were gated on CD3<sup>+</sup>,  $\gamma\delta$ TCR, V $\gamma$ 4, V $\gamma$ 4V $\delta$ 4 T cells, respectively. Representative flow plots and summarized percentage and absolute number are shown ( $n=4$  in WT/IMQ/GC group,  $n=5$  in WT/IMQ/Vas group.  $n=3$  in each group of *Tcrd*<sup>-/-</sup> mice). Data are representative of at least two independent experiments with similar results.  $****P<0.0001$ ,  $***P<0.001$ ,  $**P<0.01$   $*P<0.05$  (unpaired Student's t test). Data in the bar figures are represented as means $\pm$ SEM.

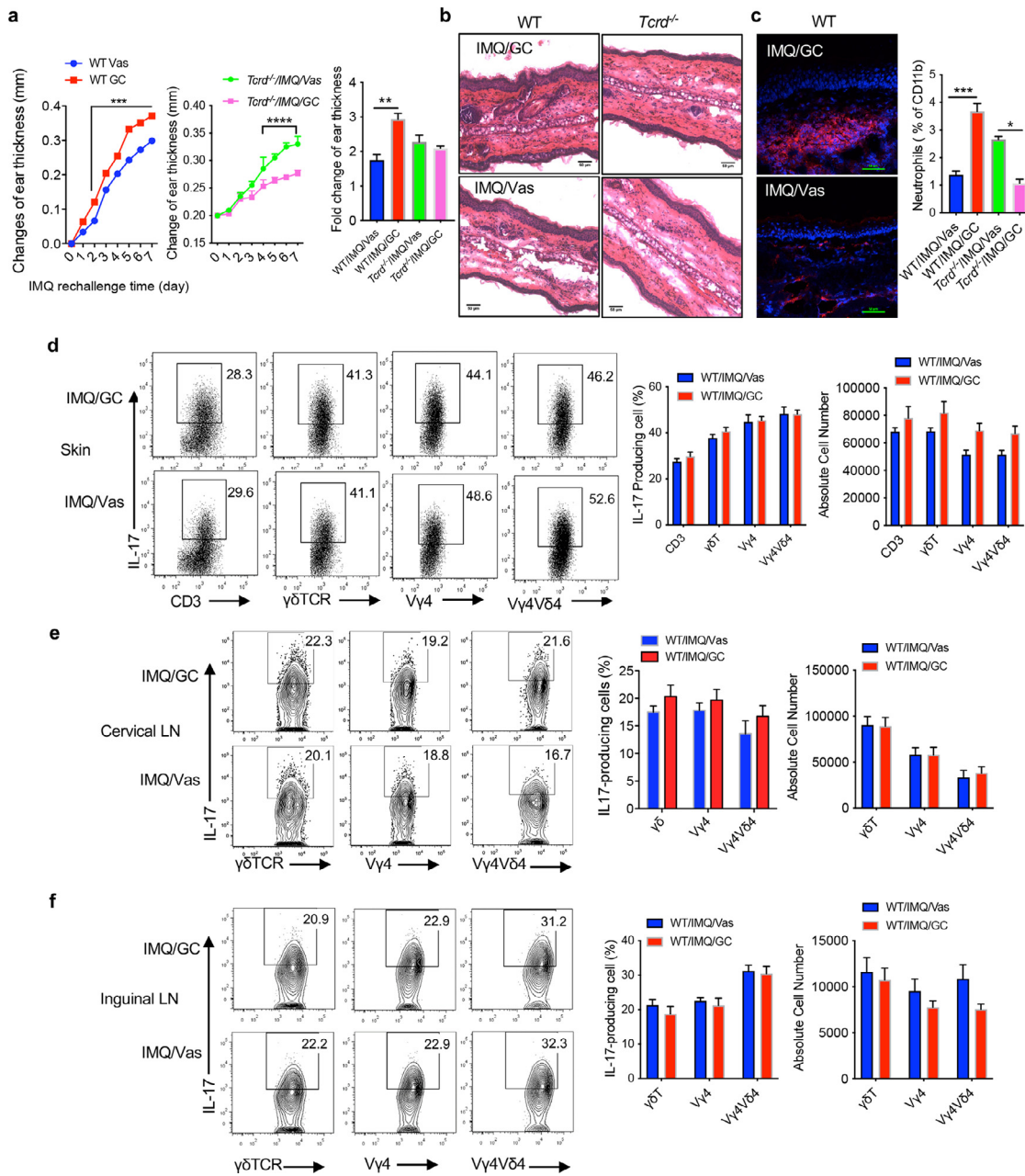


**Figure 4. Rechallenge of IMQ in mice previously treated with GC induces more severe skin inflammation.** (a) (Left and middle) Changes of ear thickness of WT mice and *Tcrd*<sup>-/-</sup> mice from Day 36 to Day 42 (ear thickness on day 35 was used as the base level). Data are combination of two experiments ( $n=8$  in each group) and represent as mean and error.  $****P<0.0001$ ,  $***P<0.001$  (unpaired Student's t test). (Right) Fold increase of ear thickness of WT mice ( $n=5$ ) or *Tcrd*<sup>-/-</sup> mice ( $n=2-3$ ). Data are the representative of at least two independent experiments with similar results.  $**P<0.01$  (one-way ANOVA). (b) Representative skin HE stained sections of WT or *Tcrd*<sup>-/-</sup> mice previously treated with or without GC on Day 42. Scale bar=50μm. (c) (Left) Representative neutrophil immunofluorescence stained skin sections of WT mice on Day 42, scale bar=50 μm. (Right) Summarized percent of neutrophils in the skin. Neutrophils were gated on CD45<sup>+</sup>CD11b<sup>+</sup> cells. The results are the combination of two experiments ( $n=10$  in each WT mice group,  $n=6$  in each *Tcrd*<sup>-/-</sup> group).  $***P<0.001$ ,  $*P<0.05$  (one-way ANOVA). (d-f) IL-17 production by dermal or LNs CD3, γδ, Vγ4, Vγ4Vδ4 T cells from skin (d), cervical LNs (e) or inguinal LNs (f) ( $n=5$ ) on day 42. Flow plots were gated on γδTCR, Vγ4, Vγ4Vδ4 T cells, respectively. Representative flow plots and summarized percentage and absolute number are shown ( $n=5$  at each WT mice). Data are representative of at least two independent experiments with similar results. (unpaired Student's t test). Data in the bar figures are represented as means±SEM.

mice. IL-17 production from CD3<sup>+</sup> T cells and  $\gamma\delta$  T cells in the skin was similar between GC-treated and Vas control mice (Figure 4d). This was for both frequency and absolute number. No difference was noticed for  $\gamma\delta$ T17 cells in the skin draining and distant LNs between these two groups (Figure 4e, 4f). This was in sharp contrast to the significant increase of these cells before IMQ re-challenge (Figure 3e and 3f). These data suggest that  $\gamma\delta$ T17 cells accumulated in the skin draining and distant LNs from previously GC-treated mice may migrate back to the skin leading to the increased severity of skin inflammation.

To further determine the critical role of  $\gamma\delta$  T cell trafficking in mediating the heightened skin inflammation in previously GC treated mice, we sorted  $\gamma\delta$  T cells from skin draining LNs of previously GC-treated or Vas control mice on day 35. These cells were adoptively transferred into naïve mice and recipient mice were then applied IMQ on the ears (Figure S4a). As shown in Figure S4b, mice received  $\gamma\delta$  T cells from GC-treated mice had significantly increased epidermal thickness than those from control mice starting at day 4 post transfer. In addition, the percentages of IL-17-producing dermal CD3<sup>+</sup>, V $\gamma$ 4 T cells, and V $\gamma$ 4V $\delta$ 4 T cells were all increased in these mice (Figure S4c) while no difference was noticed in the draining and distant LNs (Figure S4d). These data suggest the causative role of  $\gamma\delta$  T cells in inducing this heightened skin inflammation. To examine the specificity of IMQ rechallenge in previously GC-treated or Vas control mice, the second IMQ application was done on the different ear from primary IMQ treatment (Figure S4e). Mice challenged with IMQ on the same ear were used as control. Consistent with previous results, GC-treated mice rechallenged with IMQ on the same ear showed the increased epidermal thickness compared to Vas control mice (Figure S4f). However, GC-treated mice received the second IMQ application on the opposite ear showed significantly decreased epidermal thickness compared to Vas control mice (Figure S4f). In addition, the overall percentages of IL-17 production from CD3, total  $\gamma\delta$ , V $\gamma$ 4, and V $\gamma$ 4V $\delta$ 4 T cells in the skin from these mice were substantially lower than those from mice received the second IMQ on the same ears (Figure S4g). In contrast, IL-17-producing V $\gamma$ 4 and V $\gamma$ 4V $\delta$ 4 T cells were still higher in the draining LNs of these mice received IMQ rechallenge on the opposite ears (Figure S4h). These data indicate that the heightened skin inflammation upon GC treatment is induced in the same lesional skin, reminiscent of human psoriasis recurrence.

#### CCR6 is essential for $\gamma\delta$ T17 cell dynamic trafficking between LNs and dermis

Previous studies have shown that CCR2 and CCR6 play critical roles in  $\gamma\delta$ T17 cell migration during skin inflammation.<sup>20–22</sup> We thus used home-bred WT, *Ccr2*<sup>-/-</sup>,

and *Ccr6*<sup>-/-</sup> mice to examine whether  $\gamma\delta$ T17 cell trafficking is responsible for the observed phenotype. In addition, three strains of mice from the same facility were used to eliminate the potential impact of skin microbiota.<sup>23–25</sup> Although upon GC treatment, all strains of mice showed decreased ear thickness, significant differences were recorded between WT and *Ccr6*<sup>-/-</sup> mice (Figure 5a) but *Ccr2*<sup>-/-</sup> mice did similarly as WT mice (Figure 5b). Neutrophil accumulation in GC-treated WT and *Ccr2*<sup>-/-</sup> mice were also significantly lower than that in Vas control mice but there was no difference in *Ccr6*<sup>-/-</sup> mice (Figure 5c). In the skin, IL-17 production from total CD3<sup>+</sup> T cells,  $\gamma\delta$ T cells, V $\gamma$ 4 T cells, and V $\gamma$ 4V $\delta$ 4 T cells was all significantly decreased upon GC treatment (Figure 5d). However, the increased IL-17 production from these cells in the draining and distant LNs was completely abrogated in *Ccr6*<sup>-/-</sup> mice (Figure 5e). In fact, GC-treated *Ccr6*<sup>-/-</sup> mice had significantly lower IL-17 production than Vas control (Figure 5e). Similarly, upon IMQ rechallenge in these pretreated mice, both WT and *Ccr2*<sup>-/-</sup> mice received GC treatment previously showed similar increased changes of ear thickness (Figure 5f and data not shown). However, this phenotype was abrogated in *Ccr6*<sup>-/-</sup> mice and *Ccr6*<sup>-/-</sup> mice previously treated with GC had significantly decreased epidermal thickness as compared to Vas treated control *Ccr6*<sup>-/-</sup> mice (Figure 5f). Histology also revealed similar phenotype (Figure 5g). Taken together, these data suggest that CCR6 deficiency abrogates  $\gamma\delta$ T17 trafficking from affected skin to the draining and distant LNs and vice versa.

#### Inhibition of lymphocyte egress abrogates $\gamma\delta$ T17 cell trafficking and subsequent skin inflammation

Having demonstrated critical roles of  $\gamma\delta$ T17 cell trafficking in skin inflammation, we thought inhibition of this migration may provide an effective approach to control inflammation. A small molecule FTY720 is the FDA approved drug that inhibits lymphocyte egress from lymphoid tissues via downregulating sphingosine-1 phosphate receptor (S1PR) for multiple sclerosis treatment.<sup>26</sup> To foster potential clinical translation in human psoriasis patients, we used FTY720 on day 35 before IMQ re-challenge. Administration of FTY720 completely abrogated enhanced ear thickness in previously GC-treated mice upon IMQ re-challenge (Figure 6a) and the changes of ear thickness were significantly lower in GC-treated mice compared to Vas control mice. Similarly, increased neutrophil accumulation was abrogated (Figure 6a). In addition, IL-17 production from CD3<sup>+</sup> T cells and total  $\gamma\delta$ T cells in the skin was significantly decreased in mice treated with FTY720 (Figure 6b). This was not only for GC-treated mice but also for Vas control mice. FTY720 administration before IMQ re-challenge led to an even more marked accumulation of  $\gamma\delta$ T17 and V $\gamma$ 4T17 in the skin

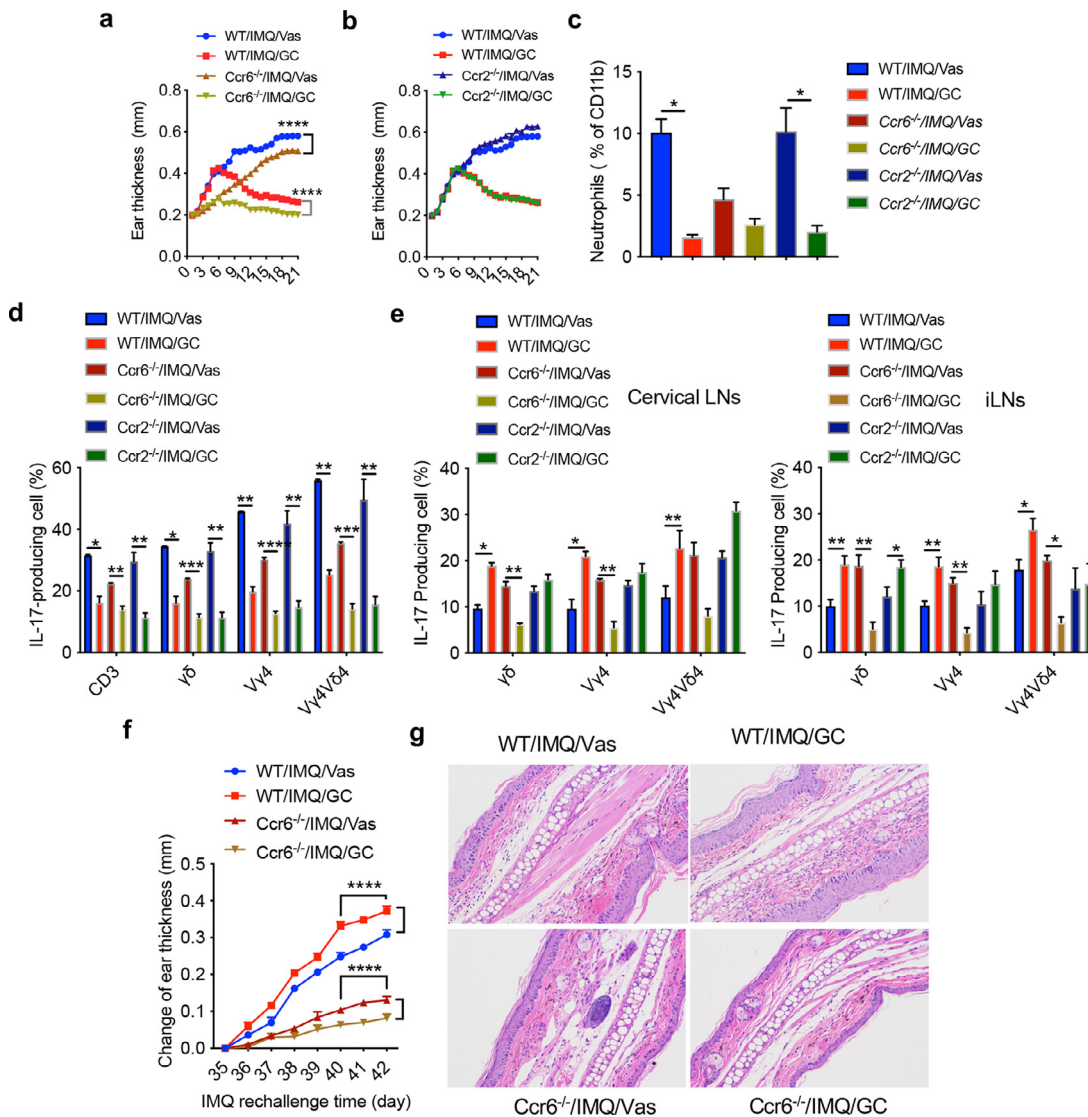


**Figure 5.**  $\gamma\delta$ T17 trafficking induced by GC treatment is dependent on CCR6. (A, B) Ear thickness of WT and *Ccr6*<sup>-/-</sup> (a) or *Ccr2*<sup>-/-</sup> mice (b, n=5) from Day 1 to Day 21. Data are the representative of at least two independent experiments with similar results. Data represent as mean and error. \*\*\*\**P*<0.0001 (two-way ANOVA). (c) Summarized neutrophil percentages. Neutrophils were gated on CD45<sup>+</sup>CD11b<sup>+</sup> cells. Data are the representative of at least two independent experiments with similar results (n=3 in each group). \**P*<0.05 (one-way ANOVA). (d, e) Summarized IL-17 production by skin CD3<sup>+</sup>, dermal or LNs  $\gamma\delta$ T, V $\gamma$ 4, V $\gamma$ 4V $\delta$ 4 T cells of WT, *Ccr6*<sup>-/-</sup> and *Ccr2*<sup>-/-</sup> mice from skin (d), cervical LNs (e, Left) or inguinal LNs (e, Right) on day 21 (n=6 in WT group, n=5 in *Ccr6*<sup>-/-</sup>/IMQ/Vas group, n=6 in *Ccr6*<sup>-/-</sup>/IMQ/GC group, n=3 in *Ccr2*<sup>-/-</sup> group). Data are representative of at least two independent experiments with similar results, \*\*\**P*<0.001, \*\**P*<0.01, \**P*<0.05, (two-way ANOVA). (f) Ear thickness of WT and *Ccr6*<sup>-/-</sup> mice rechallenge with IMQ from Day 35 to Day 42. Data represent as mean and error. \*\*\*\**P*<0.0001 (two-way ANOVA). (g) Representative HE stained skin sections from WT or CCR6 KO mice rechallenge with IMQ on day 42. Data in the bar figures are represented as means $\pm$ SEM.

draining LNs (Figure 6c left) while these cells were drastically decreased in the distant LNs (Figure 6c right). The substantial decreased in these cells was also observed in Vas control mice. These data suggest that

following expansion in the draining LNs, inhibition of  $\gamma\delta$ T17 cell egress from LNs abrogates their trafficking to the affected skin leading to significantly reduced skin inflammation.

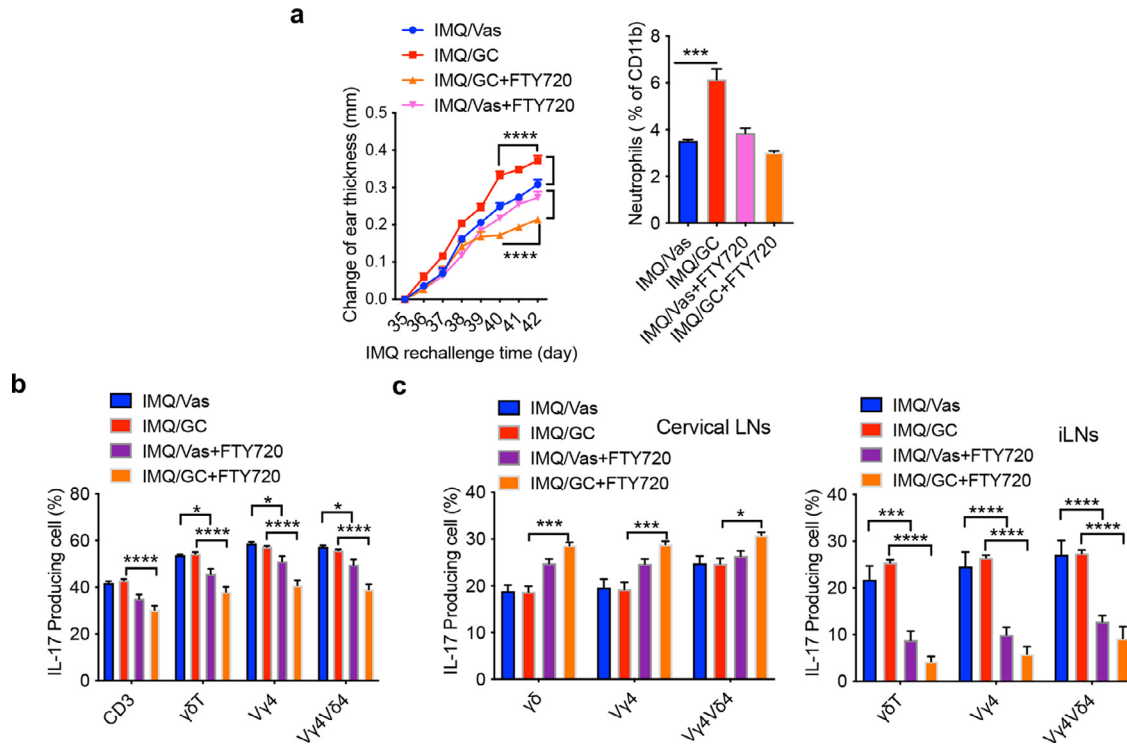


**Figure 6. FTY720 treatment inhibits  $\gamma\delta$ T17 cell trafficking leading to reduced skin inflammation and epidermal thickness.** (a) Left. Changes of ear thickness from Day 35 to Day 42 ( $n=5$  in IMQ/Vas, IMQ/GC and IMQ/GC/FTY720 group,  $n=4$  in IMQ/Vas/FTY720 group). Data represent as mean and error. \*\*\*\* $P<0.0001$  (two-way ANOVA). Right. Summarized neutrophil percentages. Cells were gated on  $CD45^+CD11b^+$  cells ( $n=3$  in IMQ group,  $n=4$  in IMQ/FTY720 group). \*\*\* $P<0.001$  (one-way ANOVA). (b-c) Summarized IL-17 production by  $CD3^+$ , dermal or LNs  $\gamma\delta$ T,  $V\gamma 4$ T,  $V\gamma 4V\delta 4$  T cells from skin (b), cervical LNs (c, Left) or inguinal LNs (c, Right) on day 42. Data are representative of at least two independent experiments with similar results ( $n=3$  in IMQ group,  $n=4$  in IMQ/FTY720 group). \*\*\*\* $P<0.0001$ , \*\*\* $P<0.001$ , \* $P<0.05$  (two-way ANOVA). Data in the bar figures are represented as means $\pm$ SEM.

## Discussion

In this study, we provide evidence to suggest that dynamic trafficking of pathogenic  $\gamma\delta T_{17}$  cells plays a critical role in the mechanisms underlying psoriasis recurrence in a mouse model of psoriasis-like dermatitis. Using skin tissues from psoriatic patients during the different disease stages, we discover that many genes and pathways related to psoriasis pathogenesis are associated with different disease statuses. Among these pathways, chemokines/chemokine receptors appear to be a dominant pathway, particularly, CCL20-CCR6 axis. Chemokine CCL20 is considered a potential biomarker for disease severity, systemic inflammation, and vascular endothelial inflammation.<sup>27</sup> Since all T17 cells express CCR6, it is thus hypothesized that T17 cells may play a critical role in psoriasis pathogenesis and recurrence. Both innate  $\gamma\delta$  T cells and adaptive T cells are able to secrete IL-17.<sup>28</sup> Previous studies have shown that T17 cells are mainly activated and differentiated in the skin and draining LNs. In psoriasis patients, PB  $\gamma\delta$  T cells are decreased while skin  $\gamma\delta$  T cells are increased, suggesting potential trafficking of  $\gamma\delta$  T cells between an inflamed skin and periphery (16). In the current study, we found the similar  $\gamma\delta$  T cell trafficking patterns during different disease stages. Skin  $\gamma\delta$  T cells were increased in untreated lesional skin while decreased upon GC effective treatment. When disease recurred, skin  $\gamma\delta$  T cells increased again. In contrast,  $\gamma\delta$  T cells in the PB experienced an opposite wave. Thus,  $\gamma\delta$  T cell trafficking appears to be correlated with disease progression, resolution, and recurrence. It will be interesting to examine whether decrease of  $\gamma\delta$  T cell frequency in the PB over time is associated with an increased risk of psoriatic flair.

Although human psoriatic patient studies have established critical correlations between T17 cells and disease development and recurrence, it is difficult to establish the firm causative effect. Previous studies have demonstrated that CD8<sup>+</sup> T<sub>RM</sub> cells produce IL-17 and CD4<sup>+</sup> T<sub>RM</sub> cells secrete IL-22 upon stimulation.<sup>29</sup> However, a recent clinical study using skin biopsies from patients received three different biologics with overall good drug response showed a reduction in IL-17-producing CD103<sup>-</sup> T cells.<sup>30</sup> No changes were observed in CD103<sup>+</sup> T<sub>RM</sub> cells. Given these perplexing results, it is thus desirable to use an animal model which can mimic clinical disease progression and treatment response. In this study, we used a well-established IMQ-induced psoriasis-like skin inflammation model and showed that GC treatment effectively ameliorated skin inflammation. Rechallenge of these mice on the same site by IMQ induced accelerated skin inflammation, resembling clinical disease relapse in psoriatic patients. In this model system, we showed that dermal  $\gamma\delta T_{17}$  cells are associated with different skin inflammation status. In IMQ-induced acute skin inflammation, dermal

$\gamma\delta T_{17}$  cells were increased while they were decreased upon GC effective treatment. Unexpectedly, these innate  $\gamma\delta T_{17}$  cells were not eliminated as a result of effective GC treatment. In contrast,  $\gamma\delta T_{17}$  cells were significantly increased in skin draining and distant LNs, suggesting potential redistribution of dermal  $\gamma\delta T_{17}$  cells. This is reminiscent to the previous study showing V $\gamma$ 4T17 cells trafficking to distant skin and inducing the secondary IL-17-driven inflammation.<sup>16</sup> More importantly, adoptively transferred  $\gamma\delta$  T cells from LNs of previously GC-treated mice into naïve mice also induced severe skin inflammation. These data suggest a causative effect of  $\gamma\delta$  T cells in mediating this phenotype. Interestingly, these GC-treated mice received the second IMQ application on the different site did not phenocopy these effects, reminiscent of human psoriasis recurrence. Our results provide unequivocal evidence that enhanced skin inflammation in previously GC-treated mice is the consequence of dynamic trafficking of  $\gamma\delta T_{17}$  cells within the skin and skin draining and distant LNs. It is worth noting that although IMQ-induced psoriasis-like dermatitis model has been widely used, this model has its limitations such as unintended consequences of topical treatment.<sup>31</sup> In addition, rechallenge of IMQ on the same skin is different from recurrence in human psoriasis. Future studies are needed to further examine these findings in psoriasis patients during different disease stages.

We demonstrated that CCR6 but not CCR2 is required for  $\gamma\delta T_{17}$  trafficking. This is in contrast to previous studies showing that CCR2 is expressed on activated  $\gamma\delta T_{17}$  cells and is essential for their accumulation in inflamed skin.<sup>16,22</sup> CCR2 is predominantly expressed on monocytes and macrophages and is required for their homing to inflamed skin.<sup>32,33</sup> Since CCR2 is only expressed on activated  $\gamma\delta T_{17}$  cells, depletion of CCR2 on them may address the observed discrepancies. Furthermore, a previous study showed that pertussis toxin did not inhibit the migration of  $\gamma\delta$  T cells from the skin to LNs<sup>34</sup> and sphingosine-1-phosphate receptor 2 (S1PR2) was thought to play a critical role in CCR6<sup>+</sup>  $\gamma\delta$  T cell egress from the skin.<sup>35</sup> However, these studies were done in the steady conditions while skin inflammation was induced in our model. Nevertheless, our finding clearly demonstrates the critical role of CCR6 for pathogenic  $\gamma\delta T_{17}$  cell migration and suggests that CCR6 may serve as a therapeutic target for durable psoriasis treatment. Indeed, many efforts have been made to develop CCR6 specific inhibitors including CCR6 antibody, small molecule inhibitor, and CCL20 derivative that show efficacy to prevent skin inflammation<sup>36–38</sup> although randomized trials are needed to firmly support their clinical utilization. In this study, we also showed that inhibition of lymphocyte egress by FTY720 abolished  $\gamma\delta T_{17}$  trafficking thus leading to reduced skin inflammation. It is thus speculated that use of

CCR6-specific inhibitors or FTY720 during psoriasis remission phase might prevent potential disease recurrence and ameliorate psoriasisform dermatitis in this mouse model.

One intriguing question is why and how  $\gamma\delta T_{17}$  cells accumulate in the skin draining and distant LNs upon GC treatment on inflamed skin. We found that the mRNA levels of CCL20 but not CCL2 were increased in the skin draining and distant LNs from GC-treated mice. However, the increased CCL20 mRNA expression was abrogated in CCR6 KO mice (data not shown). A previous study also showed that GC treatment enhanced CCL20 release in bronchial epithelial cells.<sup>39</sup> This is in contrast to the decreased CCL20 and CCL2 mRNA levels in the skin (data not shown). These results further support the notion that CCL20-CCR6 axis plays an important role in pathogenic  $\gamma\delta T_{17}$  trafficking during skin inflammation and disease treatment. This may not be specific for GC treatment as deficiency of IL-17R leads to expanded  $\gamma\delta T_{17}$  cells in skin draining LNs and development of spontaneous skin inflammation.<sup>40</sup> In summary, our results suggest that dermal  $\gamma\delta T_{17}$  cells are decreased in the inflamed skin with ameliorated inflammation upon GC treatment. These  $\gamma\delta T_{17}$  cells are not eliminated but accumulated in the draining and distant LNs due to increased CCL20 expression. Accumulation of  $\gamma\delta T_{17}$  cells in the draining and distant LNs provides a reservoir for their future trafficking back to the skin. Upon re-exposure of the same insults on the same site, pathogenic  $\gamma\delta T_{17}$  cells can quickly migrate from LNs to the skin leading to a heightened inflammation. This dynamic trafficking between the skin and LNs is CCR6 dependent. Our findings thus provide strong impetus for inhibiting pathogenic  $\gamma\delta T_{17}$  cells redistribution as an effective treatment to prevent disease relapse in patients with psoriasis and in this psoriasis-like dermatitis mouse model.

#### Contributors

Conceptualization: JZ, JY and NL. Data curation: NL, HQ, YC, QX, XL, LW, FX, LC, CD, XH. Formal Analysis: DT, ER, JY. Writing – original draft: JY, NL and HQ. Resources: JY and JZ. Writing – review & editing: JY and JZ. All authors have read and approved the final version of the manuscript.

#### Data sharing statement

RNA-Seq data have been deposited into NCBI GEO with the accession number (GSE114729).

#### Declaration of interests

ECR received consulting fee from University of South Carolina and Marshall University and participated on a Data Safety Monitoring Board or Advisory Board of

National Library of Medicine. All other authors have declared that no conflict of interest exists.

#### Acknowledgements

The authors are grateful to Drs. Yuping Lai, Jing Wang, Ningli Li, and Honglin Wang for the helpful discussions.

#### Supplementary materials

Supplementary material associated with this article can be found in the online version at doi:[10.1016/j.ebiom.2022.104136](https://doi.org/10.1016/j.ebiom.2022.104136).

#### References

- Lowes MA, Suarez-Farinas M, Krueger JG. Immunology of psoriasis. *Annu Rev Immunol*. 2014;32:227–255.
- Nestle FO, Kaplan DH, Barker J. Psoriasis. *N Engl J Med*. 2009;361(5):496–509.
- Araujo EG, Finzel S, Englbrecht M, et al. High incidence of disease recurrence after discontinuation of disease-modifying antirheumatic drug treatment in patients with psoriatic arthritis in remission. *Ann Rheum Dis*. 2015;74(4):655–660.
- Masson Regnault M, Konstantinou MP, Khemis A, et al. Early relapse of psoriasis after stopping brodalumab: a retrospective cohort study in 77 patients. *J Eur Acad Dermatol Venereol*. 2017;31(9):1491–1496.
- Lebwohl M, Strober B, Menter A, et al. Phase 3 studies comparing brodalumab with ustekinumab in psoriasis. *N Engl J Med*. 2015;373(14):1318–1328.
- Clark RA. Gone but not forgotten: lesional memory in psoriatic skin. *J Invest Dermatol*. 2011;131(2):283–285.
- Matos TR, O'Malley JT, Lowry EL, et al. Clinically resolved psoriatic lesions contain psoriasis-specific IL-17-producing alphabeta T cell clones. *J Clin Invest*. 2017;127(11):4031–4041.
- Cheuk S, Wilken M, Blomqvist L, et al. Epidermal Th22 and Tc17 cells form a localized disease memory in clinically healed psoriasis. *J Immunol*. 2014;192(7):3111–3120.
- Clark RA. Resident memory T cells in human health and disease. *Sci Transl Med*. 2015;7(269):269rv1.
- Gallais Serezal I, Classon C, Cheuk S, et al. Resident T cells in resolved psoriasis steer tissue responses that stratify clinical outcome. *J Invest Dermatol*. 2018;138(8):1754–1763.
- Cai Y, Shen X, Ding C, et al. Pivotal role of dermal IL-17-producing gammadelta T cells in skin inflammation. *Immunity*. 2011;35(4):596–610.
- Cai Y, Fleming C, Yan J. Dermal gammadelta T cells—a new player in the pathogenesis of psoriasis. *Int Immunopharmacol*. 2013;16(3):388–391.
- Mabuchi T, Singh TP, Takekoshi T, et al. CCR6 is required for epidermal trafficking of gammadelta-T cells in an IL-23-induced model of psoriasisform dermatitis. *J Invest Dermatol*. 2013;133(1):164–171.
- Pantelyushin S, Haak S, Ingold B, et al. Rorgammata+ innate lymphocytes and gammadelta T cells initiate psoriasisform plaque formation in mice. *J Clin Invest*. 2012;122(6):2252–2256.
- Hartwig T, Pantelyushin S, Croxford AL, Kulig P, Becher B. Dermal IL-17-producing gammadelta T cells establish long-lived memory in the skin. *Eur J Immunol*. 2015;45(11):3022–3033.
- Ramirez-Valle F, Gray EE, Cyster JG. Inflammation induces dermal Vgamma4+ gammadeltaT17 memory-like cells that travel to distant skin and accelerate secondary IL-17-driven responses. *Proc Natl Acad Sci USA*. 2015;112(26):8046–8051.
- Suarez-Farinas M, Fuentes-Duculan J, Lowes MA, Krueger JG. Resolved psoriasis lesions retain expression of a subset of disease-related genes. *J Invest Dermatol*. 2011;131(2):391–400.
- van der Fits L, Mourits S, Voerman JS, et al. Imiquimod-induced psoriasis-like skin inflammation in mice is mediated via the IL-23/IL-17 axis. *J Immunol*. 2009;182(9):5836–5845.
- Laggner U, Di Meglio P, Perera GK, et al. Identification of a novel proinflammatory human skin-homing Vgamma9Vdelta2 T cell

- subset with a potential role in psoriasis. *J Immunol.* 2011;187(5):2783–2793.
- 20 Hedrick MN, Lonsdorf AS, Shirakawa AK, et al. CCR6 is required for IL-23-induced psoriasis-like inflammation in mice. *J Clin Invest.* 2009;119(8):2317–2329.
  - 21 Mabuchi T, Singh TP, Takekoshi T, et al. CCR6 is required for epidermal trafficking of gammadelta-T cells in an IL-23-induced model of psoriasisform dermatitis. *J Invest Dermatol.* 2013;133(1):164–171.
  - 22 McKenzie DR, Kara EE, Bastow CR, et al. IL-17-producing gammadelta T cells switch migratory patterns between resting and activated states. *Nat Commun.* 2017;8:15632.
  - 23 Naik S, Bouladoux N, Wilhelm C, et al. Compartmentalized control of skin immunity by resident commensals. *Science.* 2012;337(6098):1115–1119.
  - 24 Ridaura VK, Bouladoux N, Claesen J, et al. Contextual control of skin immunity and inflammation by *Corynebacterium*. *J Exp Med.* 2018;215(3):785–799.
  - 25 Cai Y, Xue F, Quan C, et al. A critical role of the IL-1beta-IL-1R signaling pathway in skin inflammation and psoriasis pathogenesis. *J Invest Dermatol.* 2019;139(1):146–156.
  - 26 Chun J, Kihara Y, Jonnalagadda D, Blaho VA. Fingolimod: lessons learned and new opportunities for treating multiple sclerosis and other disorders. *Annu Rev Pharmacol Toxicol.* 2019;59:149–170.
  - 27 Elnabawi YA, Garshick MS, Tawil M, et al. CCL20 in psoriasis: a potential biomarker of disease severity, inflammation, and impaired vascular health. *J Am Acad Dermatol.* 2021;84(4):913–920.
  - 28 Hawkes JE, Chan TC, Krueger JG. Psoriasis pathogenesis and the development of novel targeted immune therapies. *J Allergy Clin Immunol.* 2017;140(3):645–653.
  - 29 Owczarczyk Saczonek A, Krajewska-Włodarczyk M, Kasprówicz-Furmanczyk M, Placek W. Immunological memory of psoriatic lesions. *Int J Mol Sci.* 2020;21(2):625. <https://doi.org/10.3390/ijms21020625>.
  - 30 Mashiko S, Edelmayer RM, Bi Y, et al. Persistence of inflammatory phenotype in residual psoriatic plaques in patients on effective biologic therapy. *J Invest Dermatol.* 2020;140(5):1015–1025.e4.
  - 31 Hawkes JE, Gudjonsson JE, Ward NL. The snowballing literature on imiquimod-induced skin inflammation in mice: a critical appraisal. *J Invest Dermatol.* 2017;137(3):546–549.
  - 32 Vestergaard C, Just H, Baumgartner Nielsen J, Thestrup-Pedersen K, Deleuran M. Expression of CCR2 on monocytes and macrophages in chronically inflamed skin in atopic dermatitis and psoriasis. *Acta Derm Venereol.* 2004;84(5):353–358.
  - 33 Willenborg S, Lucas T, van Loo G, et al. CCR2 recruits an inflammatory macrophage subpopulation critical for angiogenesis in tissue repair. *Blood.* 2012;120(3):613–625.
  - 34 Nakamizo S, Egawa G, Tomura M, et al. Dermal Vgamma4(+) gammadelta T cells possess a migratory potency to the draining lymph nodes and modulate CD8(+) T-cell activity through TNF-alpha production. *J Invest Dermatol.* 2015;135(4):1007–1015.
  - 35 Laidlaw BJ, Gray EE, Zhang Y, Ramirez-Valle F, Cyster JG. Sphingosine-1-phosphate receptor 2 restrains egress of gammadelta T cells from the skin. *J Exp Med.* 2019;216(7):1487–1496.
  - 36 Getschman AE, Imai Y, Larsen O, et al. Protein engineering of the chemokine CCL20 prevents psoriasisform dermatitis in an IL-23-dependent murine model. *Proc Natl Acad Sci USA.* 2017;114(47):12460–12465.
  - 37 Robert R, Ang C, Sun G, et al. Essential role for CCR6 in certain inflammatory diseases demonstrated using specific antagonist and knockin mice. *JCI Insight.* 2017;2(15):e94821. <https://doi.org/10.1172/jci.insight.94821>.
  - 38 Campbell JJ, Ebsworth K, Ertl LS, et al. IL-17-secreting gammadelta T cells are completely dependent upon CCR6 for homing to inflamed skin. *J Immunol.* 2017;199(9):3129–3136.
  - 39 Zijlstra GJ, Fattahi F, Rozeveld D, et al. Glucocorticoids induce the production of the chemoattractant CCL20 in airway epithelium. *Eur Respir J.* 2014;44(2):361–370.
  - 40 Fleming C, Cai Y, Sun X, et al. Microbiota-activated CD103+ DCs stemming from microbiota adaptation specifically drive gammadeltaT17 proliferation and activation. *Microbiome.* 2017;5(1):46. <https://doi.org/10.1186/s40168-017-0263-9>.